Structure and developmental regulation of the B-lymphoid tyrosine kinase gene blk. J Biol Chem 1992;267:4815–23.
4. Hochberg MC, for the Diagnostic and Therapeutic Criteria Committee of the American College of Rheumatology. Updating the American College of Rheumatology revised criteria for the classification of systemic lupus erythematosus [letter]. Arthritis Rheum 1997;40:1725.
5. Schildkraut JM. Examining complex genetic interactions. In: Haines JL, Pericak-Vance MA, editors. Approach to gene mapping in complex human diseases. New York: Wiley-Liss; 1998. p. 379–410.
6. Ohashi J, Yamamoto S, Tsuchiya N, Hatta Y, Komata T, Matsushita M, et al. Comparison of statistical power between 2×2 allele frequency and allele positivity tables in case-control studies of complex disease genes. Ann Hum Genet 2001;65:197–206.
7. Hashimoto H, Nishimura Y, Dong RP, Kimura A, Sasazuki T, Yamanaka K, et al. HLA antigens in Japanese patients with systemic lupus erythematosus. Scand J Rheumatol 1994;23:191–6.
8. Kyogoku C, Dijstelbloem HM, Tsuchiya N, Hatta Y, Kato H, Yamaguchi A, et al. Fc receptor gene polymorphisms in Japanese patients with systemic lupus erythematosus: contribution of FCGR2B to genetic susceptibility. Arthritis Rheum 2002;46: 1242–54.
9. Chen JY, Wang CM, Ma CC, Luo SF, Edberg JC, Kimberly RP, et al. Association of a transmembrane polymorphism of Fcγ receptor IIb (FCGR2B) with systemic lupus erythematosus in Taiwanese patients. Arthritis Rheum 2006;54:3908–17.
10. Komata T, Tsuchiya N, Matsushita M, Hagiwara K, Tokunaga K. Association of tumor necrosis factor receptor 2 (TNFR2) polymorphism with susceptibility to systemic lupus erythematosus. Tissue Antigens 1999;53:527–33.
11. Horiuchi T, Kiyohara C, Tsukamoto H, Sawabe T, Furugo I, Yoshizawa S, et al. A functional M196R polymorphism of tumour necrosis factor receptor type 2 is associated with systemic lupus erythematosus: a case-control study and a meta-analysis. Ann Rheum Dis 2007;66:320–4.
12. Kawasaki A, Tsuchiya N, Ohashi J, Murakami Y, Fukazawa T, Kusaoi M, et al. Role of APRIL (TNFSF13) polymorphisms in the susceptibility to systemic lupus erythematosus in Japanese. Rheumatology (Oxford) 2007;46:776–82.
13. Koyama T, Tsukamoto H, Masumoto K, Himeji D, Hayashi K, Harada M, et al. A novel polymorphism of the human APRIL gene is associated with systemic lupus erythematosus. Rheumatology (Oxford) 2003;42:980–5.
14. Kawasaki A, Kyogoku C, Ohashi J, Miyashita R, Hikami K, Kusaoi M, et al. Association of IRF5 polymorphisms with systemic lupus erythematosus in a Japanese population: support for a crucial role of intron 1 polymorphisms. Arthritis Rheum 2008;58:826–34.
15. Tahira T, Masumoto M, Kukita Y, Horiuchi T, Hayashi K. Pooling-based genomewide association study identifies loci for systemic lupus erythematosus [abstract]. Presented at the 57th Annual Meeting of the American Society of Human Genetics; 2007 Oct 24–7; San Diego, California. URL: http://www.ashg.org/cgi-bin/ashg07s/ashg07.

Muscarinic-3 acetylcholine receptor autoantibody in patients with systemic sclerosis: contribution to severe gastrointestinal tract dysmotility

Y Kawaguchi,[1] Y Nakamura,[2] I Matsumoto,[2] E Nishimagi,[1] T Satoh,[3] M Kuwana,[3] T Sumida,[2] M Hara[1]

See Editorial, p 609

[1] Tokyo Women's Medical University, Tokyo, Japan; [2] University of Tsukuba, Tsukuba, Japan; [3] Keio University, Tokyo, Japan

Correspondence to: Dr Y Kawaguchi, Institute of Rheumatology, Tokyo Women's Medical University, 10–22 Kawada-cho, Shinjuku-ku, Tokyo 162-0054, Japan; y-kawa@ior.twmu.ac.jp

Accepted 22 August 2008
Published Online First 31 August 2008

ABSTRACT

Objective: Patients with systemic sclerosis (SSc) complicated by severe gastrointestinal tract (GIT) dysmotility at an early stage are difficult to treat and mortality is high. To clarify the pathogenesis of GIT involvement, the occurrence of autoantibody was investigated for muscarinic-3 acetylcholine receptor (M3R) in patients with SSc.

Methods: Fourteen patients with severe GIT involvement (malabsorption syndrome and/or pseudo-obstruction) within 2 years of SSc onset (group 1) were enrolled in the present study. Sixty-two patients with SSc without severe GIT involvement within 2 years of onset (group 2) were also recruited, along with 70 healthy control subjects. Using an established enzyme immunoassay (EIA) system detecting autoantibody against the second loop domain of M3R, the presence of an anti-M3R antibody was examined in SSc patients.

Results: The mean optical density (OD) titres of group 1 were significantly higher than those of group 2 (0.65 (SD 0.58) vs 0.066 (SD 0.13), $p<0.001$). The positivity of anti-M3R antibody was significantly higher in group 1 than in group 2 (9/14 vs 3/62, $p = 2.5 \times 10^{-6}$ by Fisher's exact test). The cutoff OD was calculated from the EIA reaction of the 70 healthy controls (the mean value plus 2 SD was 0.295).

Conclusion: The findings indicated that anti-M3R antibody very frequently appears in patients with SSc, which is accompanied by severe GIT involvement, suggesting that M3R-mediated enteric cholinergic neurotransmission may provide a pathogenic mechanism for GIT dysmotility in SSc.

Systemic sclerosis (SSc) is a connective tissue disease, characterised by tissue fibrosis of multiple organs, microvascular damage and autoimmunity. More than approximately 90% of patients with SSc develop gastrointestinal tract (GIT) involvement, leading to dysmotility.[1] Because the pathological hallmark of GIT involvement in SSc is smooth muscle fibrosis, it was believed that GIT manifestations could result from tissue fibrosis. Severe manifestations such as malabsorption, repeated episodes of pseudo-obstruction, severe constipation, megacolon and malabsorption syndrome are rarely observed in patients with SSc. We recently demonstrated that severe GIT involvement in early stage SSc (less than 2 years from onset) was seen in 14 out of a consecutive 302 patients (4.6%).[2] The manifestations were significantly associated with diffuse cutaneous type SSc and myositis, suggesting that the changes in smooth muscle atrophy and fibrosis might be involved in severe GIT involvement.

On the other hand, neuropathic disturbance, especially cholinergic neurotransmission, possibly affects GIT dysmotility in SSc. Contractile activity of the GIT is controlled predominantly by intrinsic neurons in the myenteric plexus.[3] Acetylcholine, acting predominantly via the muscarinic-3 receptor (M3R), is the principal excitatory neurotransmitter regulating GIT motility. Antibodies blocking M3R would therefore be expected to inhibit excitatory enteric neurotransmission and cause dysmotility. A previous study by Goldblatt *et al*[4] demonstrated that M3R-mediated contractions were inhibited by Ig fractions derived from the sera of seven patients with SSc. However, the question of whether such anti-M3R antibodies are present in patients with SSc and whether they are associated with severe GIT involvement remains to be answered fully. Our previous report found that eight out of 14 patients with SSc and severe GIT involvement had associated autoantibodies linked to myositis (anti-U3-snRNP, anti-signal recognition particle, anti-Ku and anti-U1 snRNP); however, in the other six patients no autoantibodies except antinuclear antibody were detected.[2] We hypothesised that the anti-M3R antibody might be present in patients with SSc and severe GIT involvement and might provoke severe GIT dysmotility.

In the present study, we explored the presence of the anti-M3R antibody in patients with SSc using an enzyme immunoassay (EIA) system reported previously, and we estimated the association of anti-M3R antibody with clinical manifestations of SSc.

PATIENTS AND METHODS

Patients

Seventy-six patients with SSc who fulfilled the criteria of the American College of Rheumatology[5] were recruited for the present study. All patients were Japanese and were classified as having diffuse cutaneous SSc or limited cutaneous SSc according to the classification of LeRoy *et al*.[6] Patients with Sjögren's syndrome (SS) who fulfilled the European consensus criteria[7] were excluded from this study. Skin thickness was assessed using the modified Rodnan total skin thickness score (maximum possible score 51).[8] According to a disease severity scale established by Medsger *et al*,[9] severe GIT involvement was defined as the presence of malabsorption syndrome, episodes of pseudo-obstruction and/or the need for parenteral

Ann Rheum Dis 2009;68:710–714. doi:10.1136/ard.2008.096545

Table 1 Clinical features of patients with SSc in this study

Characteristics	Group 1 (n = 14)	Group 2 (n = 62)
Age, median (range), years	45 (26–71)	48 (28–77)
Female, no (%)	12 (85.7)	61 (98.3)
TSS, median (range)	12 (2–31)	14 (4–46)
Cutaneous type, no (%)		
Limited	4 (28.6)	26 (41.9)
Diffuse	10 (71.4)	36 (58.1)
Average duration of follow-up, months	64.3	82.7
Organ involvement, no (%)		
Interstitial lung disease	2 (14.3)*	28 (45.2)
Cardiac involvement	1 (7.1)	9 (14.5)
Scleroderma renal crisis	0	2 (3.2)
Myositis	6 (42.9)**	7 (11.3)
Gastrointestinal involvement	14 (100)**	43 (69.3)
Antinuclear antibody, no (%)	12 (85.7)	62 (100)
Antitopoisomerase-I antibody, no (%)	2 (14.3)	24 (38.7)
Anticentromere antibody, no (%)	0	9 (14.5)
Anti-U1 snRNP antibody, no (%)	1 (7.1)	4 (6.5)
Anti-SS A antibody, no (%)	0	2 (3.2)
Anti-SS B antibody, no (%)	0	0

Group 1 consisted of systemic sclerosis (SSc) patients who developed severe gastrointestinal tract (GIT) involvement within 2 years of the first symptom of SSc; group 2 consisted of the remaining SSc patients. Gastrointestinal involvement included oesophageal, gastric and intestinal involvement irrespective of the severity. SS, Sjögren's syndrome; TSS, modified Rodnan total skin thickness score. *p = 0.04, **p = 0.01 by Fisher's exact test.

hyperalimentation. In the present study, we defined group 1 as SSc patients who developed severe GIT involvement within 2 years of their first SSc symptom (except Raynaud's phenomenon); group 2 was SSc patients who were not in group 1. All SSc patients were followed for at least 2 years. This study was approved by the ethics committee of the Institute of Rheumatology, Tokyo Women's Medical University, Japan.

Gastroesophageal reflux disease was ascertained by barium oesophagography using a multiphasic cine technique and oesophagitis was estimated with a gastrofiberscope. Interstitial lung disease was assessed by chest radiography, high-resolution computed tomography of the chest and pulmonary function testing. Pulmonary arterial hypertension was defined as a mean pulmonary artery pressure of 25 mm Hg or more and a pulmonary capillary wedge pressure of 15 mm Hg or less at rest. Scleroderma renal crisis was defined as malignant arterial hypertension and/or rapidly progressive renal failure and/or microangiopathic haemolytic anaemia. The diagnosis of myositis related to SSc was based on the clinical findings of muscular symptoms such as bilateral muscle weakness, elevated creatine kinase or aldolase levels and electromyographic and/or magnetic resonance imaging abnormalities. However, a patient with polymyositis or dermatomyositis who fulfilled definite or probable criteria of the classification by Bohan and Peter[10 11] was excluded from this study. Serum samples were also obtained from 70 healthy subjects whose mean age was 32 years (range 20–63 years).

Detection of antinuclear antibodies

All patients in this study were tested for antinuclear antibody using indirect immunofluorescence and HEp-2 cells as the antigen substrate (FANAwell autoantibody kit; Iatron Laboratories, Tokyo, Japan). The presence of anticentromere antibodies (CENP) was determined by the distinctive indirect immunofluorescence pattern on HEp-2 cells and by EIA (MESACUP-2 test; Medical and Biological Laboratories, Nagoya, Japan). Antitopoisomerase I and anti-U1 snRNP antibodies (referred to as Topo I and U1RNP) were determined by double immunodiffusion against calf thymus extracts using commercially available kits (Medical and Biological Laboratories). Only in group 1 were RNA and protein immunoprecipitation assays carried out to identify additional SSc-related and myositis-related autoantibodies, such as anti-RNA polymerase I/III, anti-U3 snRNP (U3RNP), anti-Th/To, anti-PM-Scl, anti-Ku (Ku), anti-aminoacyl transfer RNA synthetase, and anti-signal recognition particle antibodies.[12]

Detection of anti-M3R antibody

Anti-M3R antibody was measured by an EIA method described previously.[13 14] Briefly, a 25-mer peptide (KRTVPPGECFIQFLSEPTITFGTAI, 213–237 aa) corresponding to the sequence of the second extracellular loop domain of the human M3R was synthesised (Sigma-Aldrich Japan, Ishikari, Japan). A 25-mer peptide (SGSGSGSGSGSGSGSGSGSGSGS) was also synthesised as a negative control (Sigma-Aldrich Japan). The peptide solution (100 µl/well at 10 µg/ml) was adsorbed onto a Nunc-Immuno plate (Nalge Nunc International, Rochester, New York, USA) overnight at 4°C. Serum at 1 : 50 dilution was incubated for 2 h at 37°C. The plates were then washed twice with 0.05% Tween 20 in phosphate-buffered saline (PBS), and 100 µl alkaline phosphatase-conjugated goat anti-human IgG (American Qualex, San Clemente, California, USA) diluted 1 : 1000 in PBS was added. Plates were kept at room temperature for 1 h. After three washes, 100 µl p-nitrophenyl phosphate solution was added. Plates were incubated for 30 minutes at room temperature, and the optical density (OD) at 405 nm was measured by plate spectrophotometry (Bio-Rad Laboratories, Hercules, California, USA). OD was used to express the titre of anti-M3R antibody. Measurements were performed in triplicate and standardised between experiments. To determine the normal range of this EIA system, we measured OD using sera from 70 healthy normal Japanese individuals. The normal range was less than 0.295, which was defined by mean plus 2 SD.

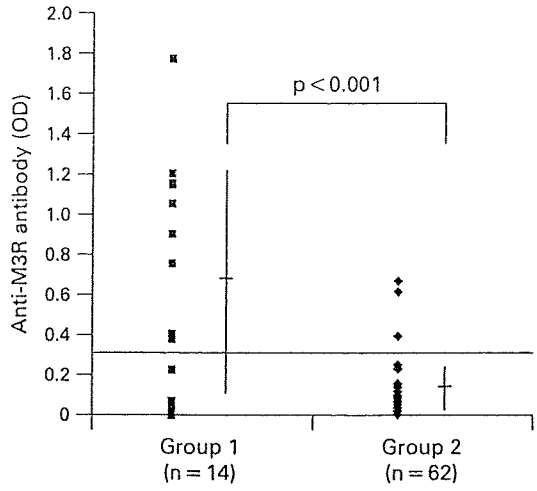

Figure 1 Anti-muscarinic-3 acetylcholine receptor (M3R) antibody in patients with systemic sclerosis (SSc). Anti-M3R antibody was determined by an enzyme immunoassay system described in the Patients and methods section. A normal value was less than 0.295, which was defined by the mean value plus 2 SD of optical density (OD) in healthy controls (n = 70). Group 1 consisted of patients with SSc complicated with severe gastrointestinal tract (GIT) involvement within 2 years of the onset and group 2 consisted of patients with SSc in the absence of severe GIT involvement within 2 years of the onset.

Statistical analysis

Frequencies of autoantibodies and clinical manifestations were evaluated by Fisher's exact test and the difference of the titres of anti-M3R antibody was estimated using the Mann–Whitney U test. The differences were considered significant at $p<0.05$.

RESULTS

Measurement of anti-M3R antibody in patients with SSc

Fourteen patients with SSc were included in group 1 and the clinical manifestations of group 1 and group 2 patients are shown in table 1.

The complications of myositis and GIT involvement were significantly more frequent in group 1 compared with group 2, but interstitial lung disease was significantly less frequent in group 1. As shown in fig 1, the titres of anti-M3R antibody were significantly higher in group 1 than in group 2 (0.65 (SD 0.58) vs 0.066 (SD 0.13), $p<0.001$). The titres of anti-M3R antibody in group 1 were also significantly higher than those in healthy controls (0.135 (SD 0.080), n = 70, $p<0.01$), but there was no significant difference in the titres of anti-M3R antibody between group 2 and healthy controls. All group 1 patients are described in table 2. In addition to the anti-M3R antibody, we estimated various SSc and myositis-related autoantibodies by RNA and protein immunoprecipitation assay. All patients had anti-M3R antibody and/or myositis-related antibodies (anti-M3R antibody alone, six patients; anti-M3R and myositis-related antibodies, three patients; myositis-related antibodies alone, five patients) as shown in table 2.

Clinical features in patients with SSc having anti-M3R antibody

We explored the frequencies of pseudo-obstruction and malabsorption in patients with SSc and severe GIT involvement. In patients with anti-M3R antibody, four patients had pseudo-obstruction, four patients had malabsorption and one patient had both pseudo-obstruction and malabsorption, as shown in table 3. Pneumatosis cystoides intestinalis is a rare complication of the most severe intestinal involvement, which affected two patients with anti-M3R antibody. In contrast, five patients with SSc and severe GIT involvement who did not have anti-M3R antibody exhibited pseudo-obstruction alone.

Among all 76 patients with SSc, 12 patients had anti-M3R antibody as shown in fig 1 (nine in group 1, three in group 2). Detailed clinical features of patients with SSc in the presence and absence of anti-M3R antibody are shown in table 4. GIT involvement was significantly more common in patients with anti-M3R antibody than in patients without anti-M3R antibody (100% vs 67.2%, $p = 0.03$; table 4). Conversely, in CENP-positive patients with SSc, the number of patients with anti-M3R antibody was significantly lower than the number of patients without anti-M3R antibody (0% vs 37.5%, $p = 0.01$; table 4).

DISCUSSION

In the present study, we have shown that patients with SSc with severe GIT involvement within 2 years from the onset of the disorder have anti-M3R antibody at a strikingly high frequency (9/14, 64%). This is the first report demonstrating the

Table 2 Summary of autoantibodies detected in 14 patients with SSc and severe GIT involvement (group 1)

Patient no	Anti-M3R antibody	Titre of anti-M3R antibody	ANA titre	ANA pattern	ANA	Clinical features
1	Positive	1.203	320	Ho	Not identified	ILD, Es
2	Positive	0.755	80	Sp	Not identified	Ca
3	Positive	1.156	2560	Ho	Not identified	Es
4	Positive	1.773	10 240	Sp, Nu	Not identified	Es
5	Positive	0.901	<40		Not identified	
6	Positive	1.054	<40		Not identified	
7	Positive	1.148	160	Nu	U3RNP	My, Es
8	Positive	0.404	20 480	Nu	U3RNP	My, Es
9	Positive	0.379	10 240	Ho, Sp	SRP	ILD
10	Negative	0.031	20 480	Nu	U3RNP	Es
11	Negative	0.000	5120	Ho, Nu	U3RNP	My
12	Negative	0.000	640	Nu	U3RNP	My
13	Negative	0.225	10 240	Ho, Nu	Topo I, Ku	My, Es
14	Negative	0.067	1280	Ho	Topo I, U1RNP	My

Interstitial lung disease (ILD), oesophagitis with gastroesophageal reflux disease (Es), cardiac involvement (Ca), and myositis (My) were mentioned as clinical features. ANA, antinuclear antibody; GIT, gastrointestinal tract; Ho, homogenous; Ku, anti-Ku antibody; M3R, muscarinic-3 acetylcholine receptor; Nu, nucleolar; Sp, speckled; SRP, antisignal recognition particle antibody; SSc, systemic sclerosis; Topo I, antitopoisomerase I antibody; U1RNP, anti-U1 snRNP antibody; U3RNP, anti-U3 snRNP antibody.

Ann Rheum Dis 2009;**68**:710–714. doi:10.1136/ard.2008.096545

Table 3 Association of anti-M3R antibody with severe GIT involvement in group 1

Group 1	Pseudo-obstruction	Malabsorption	Pseudo-obstruction plus malabsorption	PCI
Patients with anti-M3R antibodies (n = 9)	4	4	1	2
Patients without anti-M3R antibodies (n = 5)	5	0	0	0

GIT, gastrointestinal tract; M3R, muscarinic-3 receptor; PCI, pneumatosis cystoides intestinalis.

presence of autoantibody against the second extracellular loop of M3R in patients with SSc and the significant association of the anti-M3R antibody with GIT involvement in SSc. In 2002, Goldblatt *et al*[4] revealed for the first time that the Ig fraction of SSc patients exerted an inhibitory effect in M3R-mediated contraction of mouse colon smooth muscle and speculated about the presence of an autoantibody against M3R in patients with SSc. They showed that seven out of nine patients with SSc had functional antibodies inhibiting M3R-mediated enteric smooth muscle contraction. All seven of those patients had secondary SS and three out of seven patients were positive for CENP. Those results are inconsistent with ours. It is possible that the subgroup of SSc patients with severe GIT involvement in our study is distinct from the subgroup of SSc patients described by Goldblatt *et al*,[4] or that anti-M3R antibody detected in our assay is physiologically different from the Ig fraction inhibiting the M3R-mediated signal in the previous study. As far as we could find, there are no previous studies indicating the association between GIT involvement and secondary SS in patients with SSc. In 302 consecutive patients with SSc, whose clinical manifestations were described by our group in 2007, 220 patients (70%) had GIT involvement and 45 patients had secondary SS complications; 35 out of those 45 patients with both SSc and SS had GIT involvement (78%).[2] Our observations did not show the significant association between secondary SS and GIT involvement in patients with SSc.

Autoantibody against M3R was reported to contribute to SS and to autonomic dysfunction in both primary and secondary SS.[15 16] The previous study of an EIA system using the second loop sequence of M3R (213–228 aa) different from ours (213–237 aa) showed that anti-M3R antibody positivity was 66 (90%) out of 73 in primary SS patients.[15] In the study by Naito and colleagues,[13] in which the same EIA system was used as in this study, the proportions of primary and secondary SS patients positive for anti-M3R antibody were 9% and 14%, respectively. In contrast, anti-M3R antibody in the subgroup of early SSc and severe GIT involvement appeared with a markedly high frequency (9/14, 64%); interestingly, they did not have the complication of SS. These observations suggest that a conformational epitope of the enteric M3R may be different from that of the M3R in salivary and lacrimal glands, and that anti-M3R antibody against the second extracellular loop domain detected in this EIA system may be more sensitive to the M3R of the GIT than to the M3R of salivary and lacrimal glands. M3R knockout mice were recently reported by several groups.[17] Loss of M3R in mice has resulted in various overt phenotypes, attributed to the impaired responses to cholinergic signals in the smooth muscle tissues (the intestines and the bladder) and salivary glands, and the phenotypes showed a functional redundancy among the subtypes.

In SSc patients with GIT involvement, manometric studies show normal contractile amplitudes but a disrupted pattern, which suggests that the regulation of smooth muscle function rather than muscle function itself is affected, leading to the conclusion that such findings represent the enteric cholinergic mechanisms. On the other hand, little contractile or no contractile activity is seen in some patients with SSc, indicating impaired muscle function. Those findings suggest that GIT dysmotility may be attributed to two different mechanisms; one is impaired smooth muscle contraction mediated by anti-M3R antibody, another is muscle dysfunction itself. In all 14 patients with SSc and severe GIT involvement at the early stage, we found key autoantibodies, including anti-U1 snRNP,

Table 4 Clinical profiles of patients with SSc in the presence or absence of anti-M3R antibody

Characteristic	All patients (n = 76)	Patients with anti-M3R antibody (n = 12)	Patients without anti-M3R antibody (n = 64)
Age, median (range), years	47 (25–77)	53 (26–73)	47 (25–77)
Sex (female : male)	73 : 3	10 : 2	63 : 1
TSS, median (range)	13 (2–46)	10 (2–30)	10 (4–46)
Cutaneous type, no (%)			
Limited	33 (43.4)	7 (58.3)	26 (40.6)
Diffuse	43 (56.6)	5 (41.7)	38 (59.4)
Disease duration, median (range), months	30 (4–260)	24 (10–120)	36 (14–260)
Organ involvement, no (%)			
Interstitial lung disease	36 (47.3)	3 (25)	33 (51.6)
Pulmonary arterial hypertension	4 (5.2)	0	4 (6.3)
Scleroderma renal crisis	2 (2.6)	0	2 (3.1)
Myositis	13 (17.1)	2 (16.7)	11 (17.2)
Gastrointestinal involvement	55 (72.4)	12 (100)*	43 (67.2)
Antitopoisomerase-I antibody, no (%)	25 (32.9)	2 (16.7)	23 (35.9)
Anticentromere antibody, no (%)	24 (31.6)	0**	24 (37.5)
Anti-U1 snRNP antibody, no (%)	14 (18.4)	0	14 (21.9)

Gastrointestinal involvement includes oesophageal, gastric and intestinal involvement. M3R, muscarinic-3 receptor; SSc, systemic sclerosis; TSS, modified Rodnan total skin thickness score. *p = 0.03, **p = 0.01 compared with patients with SSc without anti-M3R antibody by Fisher's exact test.

anti-U3 snRNP, anti-signal recognition particle, anti-Ku and anti-M3R antibodies, which may suggest the pathogenic mechanisms for GIT dysmotility seen in patients with SSc. Another important finding in SSc patients with severe GIT involvement is the difference in clinical features between patients with and without anti-M3R antibody. All patients with malabsorption or pneumatosis cystoides intestinalis had anti-M3R antibody. This suggests that patients with anti-M3R antibody may exhibit more severe intestinal involvement than patients without anti-M3R antibody.

In conclusion, we clearly demonstrate the presence of an autoantibody against the extracellular loop of M3R in early SSc patients with severe GIT involvement. The findings in the present study strongly suggest that there are at least two major pathogenic mechanisms for severe GIT involvement in SSc patients: enteric cholinergic dysregulation caused by anti-M3R antibody and impaired smooth muscle function accompanied by myositis-related autoantibodies.

Funding: This study was supported by a systemic sclerosis research grant from the Ministry of Health, Labour and Welfare in Japan.

Competing interests: None.

Ethics approval: This study was approved by the ethics committee of the Institute of Rheumatology, Tokyo Women's Medical University, Japan.

Patient consent: Obtained.

REFERENCES

1. **Domsic R,** Fasanella K, Bielefeldt K. Gastrointestinal manifestations of systemic sclerosis. *Dig Dis Sci* 2008;**53**:1163–74.
2. **Nishimagi E,** Tochimoto A, Kawaguchi Y, Satoh T, Kuwana M, Takagi K, *et al*. Characteristics of patients with early systemic sclerosis and severe gastrointestinal tract involvement. *J Rheumatol* 2007;**34**:2050–5.
3. **Ebert EC.** Gastric and enteric involvement in progressive systemic sclerosis. *J Clin Gastroenterol* 2008;**42**:5–12.
4. **Goldblatt F,** Gordon TP, Waterman SA. Antibody-mediated gastrointestinal dysmotility in scleroderma. *Gastroenterology* 2002;123:1144–50.
5. **Subcommittee for Scleroderma Criteria of the American Rheumatism Association Diagnostic and Therapeutic Criteria Committee.** Preliminary criteria for the classification of systemic sclerosis (scleroderma). *Arthritis Rheum* 1980;**23**:581–90.
6. **LeRoy EC,** Black C, Fleischmajer R, Jablonska S, Krieg T, Medsger TA Jr, *et al*. Scleroderma (systemic sclerosis): classification, subsets and pathogenesis. *J Rheumatol* 1988;**15**:202–5.
7. **Vitali C,** Bombardieri S, Jonsson R, Moutsopoulos HM, Alexander EL, Carsons SE, *et al*. Classification criteria for Sjögren's syndrome: a revised version of the European criteria proposed by the American–European Consensus Group. *Ann Rheum Dis* 2002;**61**:554–8.
8. **Clements P,** Lachenbruch P, Siebold J, White B, Weiner S, Martin R, *et al*. Inter and intraobserver variability of total skin thickness score (modified Rodnan TSS) in systemic sclerosis. *J Rheumatol* 1995;**22**:1281–5.
9. **Medsger TA Jr,** Silman AJ, Steen VD, Black CM, Akesson A, Bacon PA, *et al*. A disease severity scale for systemic sclerosis: development and testing. *J Rheumatol* 1999;**26**:2159–67.
10. **Bohan A,** Peter JB. Polymyositis and dermatomyositis (first of two parts). *N Engl J Med* 1975;**292**:344–7.
11. **Bohan A,** Peter JB. Polymyositis and dermatomyositis (second of two parts). *N Engl J Med* 1975;**292**:403–7.
12. **Kuwana M,** Kaburaki J, Okano Y, Tojo T, Homma M. Clinical and prognostic associations based on serum antinuclear antibodies in Japanese patients with systemic sclerosis. *Arthritis Rheum* 1994;**37**:75–83.
13. **Naito Y,** Matsumoto I, Wakamatsu E, Goto D, Sugiyama T, Matsumura R, *et al*. Muscarinic acetylcholine receptor autoantibodies in patients with Sjögren's syndrome. *Ann Rheum Dis* 2005;**64**:510–11.
14. **Nakamura Y,** Wakamatsu E, Matsumoto I, Tomiita M, Kohno Y, Mori M, *et al*. High prevalence of autoantibodies to muscarinic-3 acetylcholine receptor in patients with juvenile-onset Sjögren syndrome. *Ann Rheum Dis* 2008;**67**:136–7.
15. **Kovács L,** Marczinovits I, György A, Tóth GK, Dorgai L, Pál J, *et al*. Clinical associations of autoantibodies to human muscarinic acetylcholine receptor 3 in primary Sjogren's syndrome. *Rheumatology* 2005;**44**:1021–5.
16. **Waterman SA,** Gordon TP, Rischmueller M. Inhibitory effects of muscarinic receptor autoantibodies on parasympathetic neurotransmission in Sjogren's syndrome. *Arthritis Rheum* 2000;**43**:1647–54.
17. **Matsui M,** Motomura D, Karasawa H, Fujikawa T, Jiang J, Komiya Y, *et al*. Multiple functional defects in peripheral autonomic organs in mice lacking muscarinic acetylcholine receptor gene for the M3 subtype. *Proc Natl Acad Sci U S A* 2000;**97**:9579–84.

Mod Rheumatol (2009) 19:358–365
DOI 10.1007/s10165-009-0172-2

ORIGINAL ARTICLE

A new low-field extremity magnetic resonance imaging and proposed compact MRI score: evaluation of anti-tumor necrosis factor biologics on rheumatoid arthritis

Takeshi Suzuki · Satoshi Ito · Shinya Handa · Katsumi Kose · Yoshikazu Okamoto · Manabu Minami · Taichi Hayashi · Daisuke Goto · Isao Matsumoto · Takayuki Sumida

Received: 5 December 2008 / Accepted: 23 March 2009 / Published online: 16 April 2009

Abstract Magnetic resonance imaging (MRI) is a useful tool for evaluating disease activity and therapeutic efficacy in rheumatoid arthritis (RA). However, conventional whole-body MRI is inconvenient on several levels. We have therefore developed a new low-field extremity MRI (compact MRI, cMRI) and examined its clinical utility. Thirteen RA patients treated with anti-tumor necrosis factor (TNF) biologics were included in the study. The MRI was performed twice using a 0.21-T extremity MRI system. The MRI images were scored using our proposed cMRI scoring system, which we devised with reference to the Outcome Measures in Rheumatology Clinical Trials RA MRI score (OMERACT RAMRIS). In our cMRI scoring system, synovitis, bone edema, and bone erosion are separately graded on a scale from 0 to 3 by imaging over the whole hand, including the proximal interphalangeal joint. The total cMRI score (cMRIS) is then obtained by calculating the total bone erosion score × 1.5 + total bone edema score × 1.25 + total synovitis score. In this study, one patient showed a progression of bone destruction even under low clinical activity, as assessed by the disease activity score on 28 joints (DAS28); however, another patient's cMRIS decreased concurrently with the decrease in DAS28, with the positive correlation observed between ΔDAS28 and ΔcMRIS ($R = 0.055$, $P < 0.05$). We conclude that cMRI and cMRIS are useful for assessing total disease activity and as a method linking MRI image evaluation to clinical evaluation.

Keywords Anti-TNF biologics · Bone edema · Bone erosion · Low-field extremity MRI · MRI scoring system · Rheumatoid arthritis

T. Suzuki · S. Ito · T. Hayashi · D. Goto · I. Matsumoto · T. Sumida
Division of Clinical Immunology, Doctoral Program in Clinical Sciences, Graduate School of Comprehensive Human Sciences, University of Tsukuba, Tsukuba, Ibaraki, Japan

S. Handa · K. Kose
Institute of Applied Physics, University of Tsukuba, Tsukuba, Ibaraki, Japan

Y. Okamoto · M. Minami
Department of Radiology, Institute of Clinical Medicine, University of Tsukuba, Tsukuba, Ibaraki, Japan

T. Sumida (✉)
Division of Clinical Immunology, Doctoral Program in Clinical Sciences, Graduate School of Comprehensive Human Science, University of Tsukuba, 1-1-1 Tennodai, Tsukuba, Ibaraki 305-8575, Japan
e-mail: tsumida@md.tsukuba.ac.jp

Introduction

Rheumatoid arthritis (RA) is a systemic inflammatory autoimmune disease that predominantly affects the synovial membranes of joints. Persistent inflammation or synovitis leads to pannus formation and, ultimately, bone destruction. A therapeutic window [1] does exist early in the RA course; therefore, the development of better methods for the early diagnosis and treatment of RA is one of the prime objectives of rheumatologists. Conventional radiography is currently the major tool for diagnosing RA and monitoring the progression of joint destruction. However, because this technique visualizes only late signs of preceding disease activity, other diagnostic tools, such as magnetic resonance imaging (MRI), have been the focus of increasing attention in recent years. Magnetic resonance

imaging is three- to sevenfold more sensitive than conventional radiography in terms of detecting joint erosion in early-stage RA [2, 3]. It can also detect synovitis, bone edema, and tenosynovitis that is not visible on conventional radiographic scans [4, 5]. Synovitis is among the earliest abnormalities observed in RA and is, in many cases, already apparent before a patient complains of joint pain or shows elevated serum C-reactive protein (CRP). The degree of bone marrow edema in metacarpalphalangeal (MCP) and wrist joints has recently been reported to be a more important predicator of radiographic progression in early RA than the degree of synovitis, erosion, or disease activity score based on 28 joints (DAS28) [6]. Evaluating bone edema by MRI may therefore assist clinicians in determining whether a patient should receive early and aggressive treatment to avoid subsequent joint damage.

While MRI may provide significant information about the course of RA not obtainable by conventional radiography, conventional whole-body, high-field MRI is more expensive in terms of both startup costs and maintenance fees, and it is not always convenient. In addition, claustrophobic patients and those suffering severe joint pain are sometimes unable to complete the examination. Low-field extremity MRI was recently developed to address these limitations; it is now commercially available and has been used clinically to evaluate RA. Low-field extremity MRI offers adequate performance at a lower cost and with greater comfort and convenience to the patient than conventional MRI [7, 8]. One strong disadvantage of this tool, however, is that the field of view (FOV) is too small to assess hand and wrist joints in one examination or in one sequence—and RA usually affects the wrist to proximal interphalangeal (PIP) joints. This is a major limiting factor in the success of low-field MRI for diagnosing of RA or assessing disease activity.

We have recently developed a new low-field extremity MRI system with a FOV large enough to simultaneously assess the entire wrist to PIP joint area. In the study reported here, we examined the clinical value of our low-field MRI system for assessing disease activity in RA patients treated with anti-tumor necrosis factor (TNF) biologics using the original scoring system.

Patients and methods

Patients and clinical assessments

Thirteen RA outpatients were enrolled in the study (two men and 11 women). The mean disease duration at evaluation was 6.2 years. Seven patients were treated with infliximab (IFX) and six with etanercept (ETN). Clinical disease activity was determined using the DAS28–CRP. Eleven patients had moderate or high disease activity before receiving anti-TNF biologics; the remaining patients had low clinical disease activity but showed bone destruction in the wrists, which had worsened significantly within the past year, as assessed by radiography. The IFX group also received an average methotrexate dose of 8 mg/week, with six patients also treated with prednisolone (average dose 7.1 mg/day). In the ETN group, four patients also received methotrexate (average dose 5 mg/week), and all six patients were taking prednisolone (average dose 5.3 mg/day). Table 1 presents additional sociodemographic data on these patients. All patients underwent two MRI assessments; the first was carried out at the time of starting the biologics (IFX group patients 5–7; ETN group patient 6) or within 7 and 9 months from the initial infusion of IFX and ETN (IFX group patients 1–4 and ETN group patients 1–5), respectively, and the second MRI assessment was within 8–16 months and 5–23 months from the first infusion for the respective groups.

New low-field extremity MRI system and MRI protocols

The new system is called compact MRI (cMRI). It comprises a permanent magnet, a gradient coil set, and an MRI console, generating a magnetic field strength of 0.21 T. The system occupies a total installation space of 4 m^2. The magnet is placed in an electromagnetic shield room [1.6 (W) × 2.0 (H) × 2.4 (D)] to prevent external noise. Patients sit in front of the magnet and insert one hand into the radio frequency (RF) coil for MR imaging. Coronal three-dimensional (3-D) gradient recalled echo T1-weighted images [repetition time (TR)/echo time (TE) = 50/9 ms] were obtained with an image matrix size at 512 × 384 × 32, FOV of 20.48 × 15.36 × 6.4 cm, and a scan time of 7 min and 5 s. Coronal 3D fast short tau inversion recovery (STIR) images [TR/TE/inversion time (TI) = 1000/60/100 ms] were also obtained with an image matrix size of 256 × 256 × 8, FOV at 20.48 × 20.48 × 6.4 cm, and a scan time of 8 min and 30 s. Both hands were scanned in all patients. The total examination time, including patient positioning, required about 40 min.

Image evaluation and proposed compact MRI score

Magnetic resonance imaging findings are currently scored using the RA MRI scoring system (RAMRIS) as reported in the Outcome Measures in Rheumatology Clinical Trials (OMERACT) [9]. However, the RAMRIS system requires a two-dimensional (2-D) analysis, and our cMRI system can analyze only the coronary section; consequently, RAMRIS cannot be used in our system. Our modified MRI system can visualize joints from the wrist to PIP in only one image. We

Table 1 Patients' demographics

Patient	Age (years)	Sex	Disease duration (years)	Stage[a]	Class[a]	MTX (mg/week)	PSL (mg/day)	Other DMARDs
Infliximab group								
1	51	F	1	2	2	10	10	SASP
2	58	F	5	2	1	8	0	BC
3	31	F	6	3	3	8	4	
4	48	F	11	4	3	6	15	
5	55	F	14	3	3	8	12.5	
6	30	F	2	1	1	8	4	
7	39	F	4	3	2	8	4	
Average	44.6		6.1	2	2	8	7.1	
Etanercept group								
1	68	M	3	4	2	8	5	
2	18	F	2	2	1	12	6	
3	54	M	3	3	2	4	6	SASP
4	59	F	12	4	3	0	10	SASP, ACT
5	42	F	10	2	1	0	4	
6	33	F	8	4	2	6	1	
Average	45.7		6	3	2	5	5.3	

F Female, *M* male, *MTX* methotrexate, *PSL* prednisolone, *DMARDs* disease-modifying antirheumatic drugs, *SASP* salazosulfapyridine, *ACT* Actarit, *BC* bucillamine

[a] Stage was determined according to the Steinblocker's classification, and class was determined according to the Hochberg's classification

therefore evaluated the images using our original scoring system, to obtain a compact MRI score (cMRIS) referenced to RAMRIS. The cMRIS scores the degree of bone erosion, bone marrow edema, and synovitis in both hands. In this study, the MRI images were reviewed by one radiologist, who is a Board-certified radiologist (by the authority of the Japan Radiological Society), and by more than two rheumatologists. All patients' information was blinded. Bone erosion and edema were defined using the OMERACT MRI joint pathology definition [10]. Bone erosion was defined by the presence of a sharply marginated bone region that was imaged as a loss of normal signal intensity of cortical bone and a loss of normal high signal characteristics, visible in two planes, with a cortical break seen in at least one plane on the T1-weighted image. Bone edema was defined a lesion within the trabecular bone, with ill-defined margins and signal characteristics consistent with increased water content that was imaged as high-intense signal on STIR and a low-intense signal on the T1-weighted image. Since we did not use gadolinium enhancement, synovitis was defined a high signal intensity on STIR that seemed anatomically to be the synovial area. The RAMRIS rates bone erosion from 0 to 10 by volume, while our scoring system rates bone erosion on a scale from 0 to 3 by volume. Bone edema and synovitis were scored on the same scale as RAMRIS. The PIP joints were scored by the same method used for the evaluating the MCP joints. This study evaluated 23 bones and 11 joints (Fig. 1). Bone erosion and edema were estimated in one to five MCP joints and one to five carpometacarpal (CM) joints, in two to five proximal and distal PIP joints, and in all wrist bones, except for the pisiforme, distal radius, and head of ulna. In the PIP and MCP joints, we evaluated each proximal and each distal side separately. and the score of the worse side was counted. Thus, the total estimation site of bone erosion and edema was 32. Synovitis, which was also scored on a scale from 0 to 3, was evaluated in two to five PIP joints, one to five MCP joints, and in the intercarpal and distal radioulnar joints. However, the intercarpal joint synovitis score was doubled because of its large volume. The overall score was calculated as follows: total synovitis score + 1.25 × total bone edema score + 1.5 × total bone erosion score [maximum total bone erosion score 207 (3 × 23 × 1.5 × 2), maximum total bone edema score 172.5 (3 × 23 × 1.25 × 2), maximum total synovitis score 72 {(3 × 10 + 3 × 1 × 2) × 2}; maximum cMRIS 451.5]. Further details of the scoring system are provided in Table 2.

Statistical analysis

The correlation between the changes in cMRIS (ΔcMRIS) and the DAS28–CRP (ΔDAS28) values was evaluated by Pearson's correlation coefficient test. A value of $P < 0.05$ was considered to be significant.

Results

Evaluation of DAS28-CRP

The DAS28–CRP was evaluated prior to the biologics treatment and at the time of first and second MRI

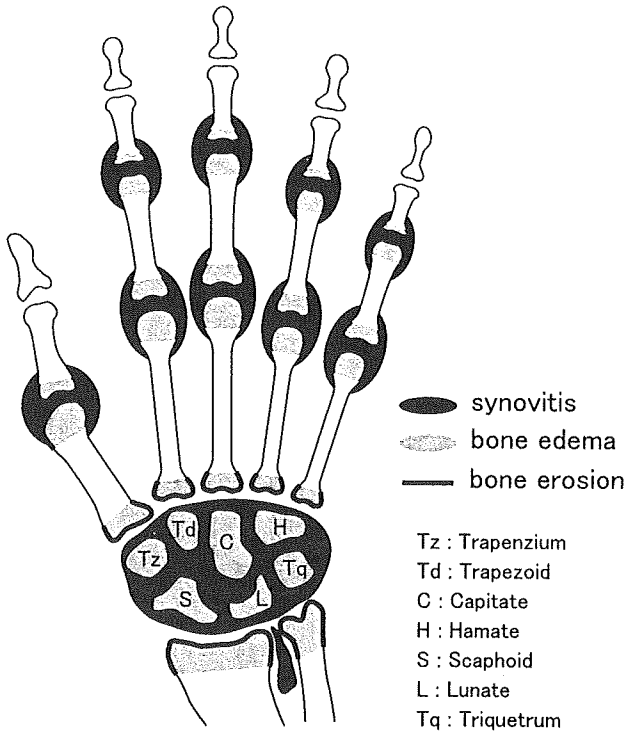

Fig. 1 Sites evaluated in calculating the compact magnetic resonance imaging (MRI) score. In this scoring system, 23 bones and 16 joints were evaluated. Pisiforme was excluded from the wrist bone evaluation. Bone erosion and edema were evaluated in 32 sites, and synovitis was evaluated in 11 sites. The score calculation is provided in detail in Table 2

examinations. All patients of both treatment groups (IFX and ETN) except one showed a moderate-to-good response, as assessed by DAS28–CRP, and none showed a recurrence of disease activity (Fig. 2).

Changes in cMRI score

Figure 2 and Table 3 provide details on the MRI scores calculated from the first and second imaging examinations for all patients. The first imaging identified seven patients with synovitis and three with bone edema in the finger joints. All patients showed bone erosion in the first and second imaging. However, erosion of the finger joints did not worsen in any of the patients included in this study, with ten of 13 patients showing an improvement over the intervening time period. Synovitis was present in the wrist joints of 12 patients at the first imaging, and although persistent, the second imaging showed improved synovitis in the wrist joints in most patients. Ten of the 13 patients showed bone edema in the wrist joint at the first imaging; by the second imaging, seven of these patients showed improvement, and three patients showed deterioration. Patient 1 of the IFX group showed remarkable joint destructions over the treatment time, while the others remained the same or showed a slight improvement.

Table 2 Compact MRI score (cMRIS) used in this study

Bone erosion	
Sites	Each wrist bone (except pisiforme), PIP (II–V), MCP (I–V), CM (I–V), carpal bones, distal radius and distal ulna, total of 23 bones, was scored separately.
Methods	Erosion was scored from 0 to 3, based on the proportion of the eroded bone relative to the assessed bone volume
	0: no erosion, 1: 1–33% of bone eroded, 2: 34–66% of bone eroded, 3: 67–100% of bone eroded.
	PIP and MCP joint was evaluated each proximal and distal side separately, and the score of the worse side was counted.
Bone edema	
Sites	Each wrist bone (except pisiforme), PIP (II–V), MCP (I–V), CM (I–V), carpal bones, distal radius and head of ulna was scored separately.
Methods	Bone edema was scored 0–3 according to the volume of edema relative to the assessed bone volume. The assessed bone volume in long bones was from the articular surface (or, if absent, its best estimated position) to a depth of 1 cm, while it was the whole bone in carpal bones
	0: no edema, 1: 1–33% of bone edematous, 2: 34–66% of bone edematous, 3: 67–100% of bone edematous.
	The PIP and MCP joints were evaluated on each proximal and distal side separately, and the score of the worse side was counted.
Synovitis	
Sites	Synovitis was assessed in 11 regions [PIP (II–V), MCP (I–V), the intercarpal and the distal radioulnar joint].
Methods	Synovitis was scored 0–3 according to the tertiles of the STIR high signal regions in the synovial compartment relative to the presumed maximum volume:
	0: normal (no synovitis), 1: mild, 2: moderate, 3: severe.
	The intercarpal joint score is doubled.
Proposed compact MRI score (cMRIS)	
cMRIS = (total bone erosion points) × 1.5 + (total bone edema points) × 1.25 + (total synovitis points) × 1	

PIP proximal interphalangea, *MCP* metacarpophalangea, *CM* carpo-metacarpa, *STIR* short tau inversion recovery

Relationship between cMRIS and DAS28-CRP

We evaluated the correlation between ΔcMRIS and ΔDAS28 in our small cohort and observed a positive correlation between the two scores ($R = 0.055$, $P < 0.05$; Fig. 3). However, one patient (IFX group patient 1) showed a very small change in the DAS28–CRP (2.66–2.83),

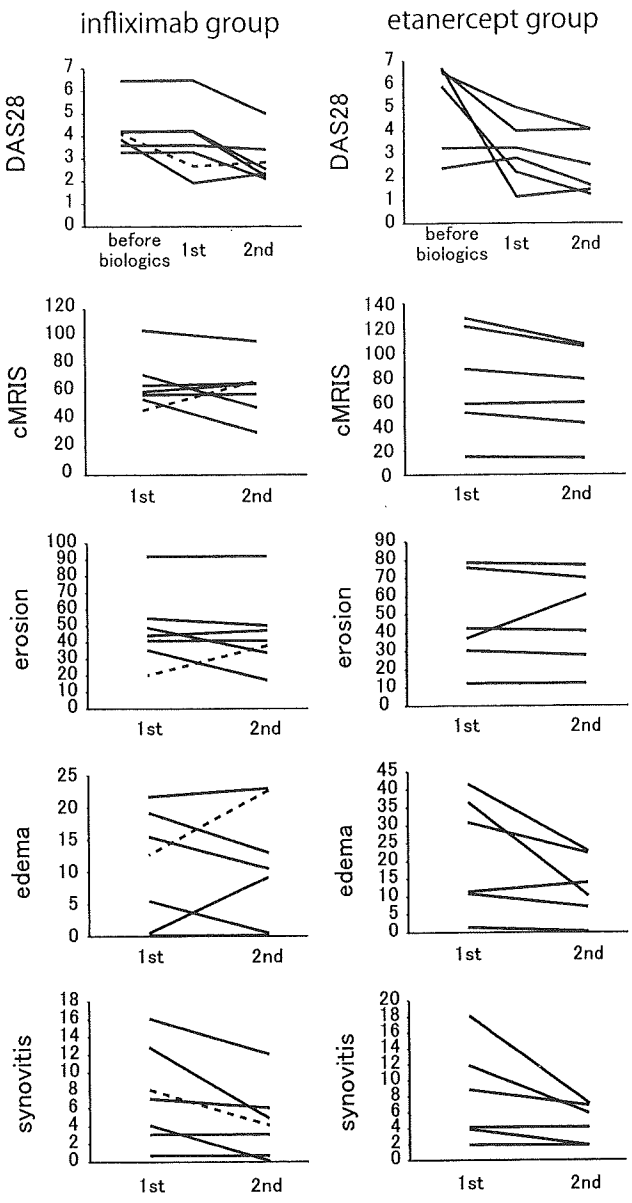

Fig. 2 Serial changes in disease activity score on 28 joints (*DAS28*) and compact MRI score (*cMRIS*) between first (*1st*) and second (*2nd*) MRI examinations. All patients except one had a good or moderate response to the biologics, and none showed increased disease activity. The cMRIS scores generally decreased or remained constant. However, one patient of the infliximab group showed an increase in cMRIS score even under low disease activity (*dotted line*)

indicating clinical remission but a marked worsening of the cMRIS (from 46.5 to 67.5).

Discussion

Rheumatoid arthritis is a chronic bone destruction disease that severely and progressively afflicts the patient's daily activities. Biologics, including TNF blockers, have recently

Table 3 Changes in compact MRI score during the present study

Patient	MRI scan	Finger joints			Wrist joints			Total cMRIS	DAS28	DAS28 at the introduction of biologics	Response
		Synovitis	Bone edema	Bone erosion	Synovitis	Bone edema	Bone erosion				
Infliximab group											
Patient 1	1st	0	0	6	7	12.5	21	46.5	1st 2.66	4.1	Good
	2nd	0	0	9	6	22.5	30	67.5	2nd 2.83		Good
	ΔcMRIS	0	0	3	−1	10	9	21	ΔDAS28 0.17		
Patient 2	1st	0	0	15	0	18.75	21	54.75	1st 4.22	4.19	No response
	2nd	0	0	9	0	12.5	9	30.5	2nd 2.51		Good
	ΔcMRIS	0	0	−6	0	−6.25	−12	−24.25	ΔDAS28 −1.71		
Patient 3	1st	1	1.25	18	2	20	22.5	64.75	1st 1.92	3.84	Good
	2nd	1	1.25	18	2	21.25	22.5	66	2nd 2.33		Good
	ΔcMRIS	0	0	0	0	1.25	0	1.25	ΔDAS28 0.41		
Patient 4	1st	6	0	6	7	0	85.5	104.5	1st 6.47	6.46	No response
	2nd	0	0	6	5	0	85.5	96.5	2nd 4.97		Moderate
	ΔcMRIS	−6	0	0	−2	0	0	−8	ΔDAS28 −1.5		

Table 3 continued

Patient	MRI scan	Finger joints			Wrist joints			Total cMRIS		DAS28	DAS28 at the introduction of biologics	Response
		Synovitis	Bone edema	Bone erosion	Synovitis	Bone edema	Bone erosion					
Patient 5	1st	0	0	4.5	4	0	49.5	58	1st	3.58	3.58	
	2nd	0	0	3	0	8.75	46.5	58.25	2nd	3.38		No response
	ΔcMRIS	0	0	−1.5	−4	8.75	−3	0.25	ΔDAS28	−0.2		
Patient 6	1st	3	0	3	13	5	42	66	1st	4.21	4.21	
	2nd	1	0	3	11	0	45	60	2nd	2.23		Good
	ΔcMRIS	−2	0	0	−2	−5	3	−6	ΔDAS28	−1.98		
Patient 7	1st	2	0	6	6	15	43.5	72.5	1st	3.27	3.27	
	2nd	0	0	6	4	10	28.5	48.5	2nd	2.09		Moderate
	ΔcMRIS	−2	0	0	−2	−5	−15	−24	ΔDAS28	−1.18		
Etanercept group												
Patient1	1st	2	0	16.5	7	11.25	13.5	50.25	1st	0.99	6.34	Good
	2nd	2	0	12	5	7.5	15	41.5	2nd	1.29		Good
	ΔcMRIS	0	0	−4.5	−2	−3.75	1.5	−8.75	ΔDAS28	0.3		
Patient 2	1st	0	0	1.5	12	36.25	36	85.75	1st	2.66	2.33	No response
	2nd	0	0	3	6	10	58.5	77.5	2nd	1.48		Moderate
	ΔcMRIS	0	0	1.5	−6	−26.25	22.5	−8.25	ΔDAS28	−1.18		
Patient 3	1st	1	1.25	7.5	1	0	4.5	15.25	1st	3.85	5.75	Moderate
	2nd	1	0	7.5	1	0	4.5	14	2nd	3.91		Moderate
	ΔcMRIS	0	−1.25	0	0	0	0	−1.25	ΔDAS28	0.06		
Patient 4	1st	0	0	6	4	41.25	70.5	121.75	1st	4.83	6.5	Moderate
	2nd	0	0	7.5	2	32.5	63	105	2nd	3.91		Moderate
	ΔcMRIS	0	0	1.5	−2	−8.75	−7.5	−16.75	ΔDAS28	−0.92		
Patient 5	1st	0	0	28.5	4	11.25	13.5	57.25	1st	2.05	6.55	Good
	2nd	0	0	28.5	4	13.75	12	58.25	2nd	1.08		Good
	ΔcMRIS	0	0	0	0	2.5	−1.5	1	ΔDAS28	−0.97		
Patient 6	1st	8	13.75	31.5	10	17.5	46.5	127.25	1st	3.09	3.09	
	2nd	3	11.25	30	4	11.25	46.5	106	2nd	2.35		Moderate
	ΔcMRIS	−5	−2.5	−1.5	−6	−6.25	0	−21.25	ΔDAS28	−0.74		

cMRIS Compact magnetic resonance imaging score, *DAS28* disease activity score in 28 joints, *CRP* C-reactive protein, *ΔcMRIS* changes in cMRIS value

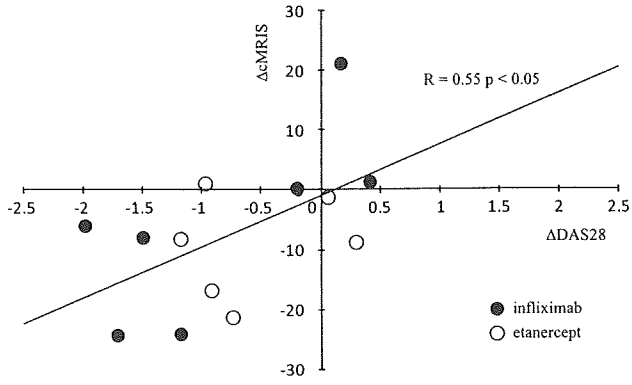

Fig. 3 Relationship between changes in the cMRIS value (ΔcMRIS) and changes in the DAS28 (ΔDAS28). ΔcMRIS and ΔDAS28 are the differences between the first and the second images. A positive correlation was observed between two evaluations ($R = 0.55$, $P < 0.05$)

raised the hope of RA sufferers of dramatic improvements in joint mobility and prognosis. The Trial of Etanercept and Methotrexate with Radiographic Patient Outcomes (TEMPO) study revealed the possibility of joint repair through treatment with ETN plus methotrexate [11]. However, many such studies used conventional radiography to evaluate bone erosion. Brown et al. [12] reported that about 96% patients treated with conventional disease-modifying antirheumatic drugs (DMARDs) achieved clinical remission according to the criteria of the American College of Rheumatology (ACR) and DAS28 score, but they still showed synovitis as assessed by MRI. The same percentage of asymptomatic patients with clinically normal joints also had synovitis based on MRI, while 46% showed bone marrow edema. In a comparative study on the therapeutic effectiveness of DMARDs and anti-TNF biologics, Martinez-Martinez et al. [13] also reported considerable synovitis based on MRI scans. This was still the case even in patients declared to be in clinical remission based on the biologics. These authors also reported no significant correlation between the improvement of clinical or laboratory data and MRI findings. Takes together, these studies stress the necessity of including an MRI examination in order to comprehensively evaluate total disease activity and joint damage in RA.

The imaging position and time needed for whole-body MRI makes it impractical for many rheumatologists to use and burdensome for the patient. Low-field extremity MRI is thus a valuable alternative that has recently become commercially available and has been tested for the diagnosis and monitoring of RA. Low-field extremity MRI improves patient comfort, is cost-effective for the institute, and yields equivalent results to whole-body MRI in terms of RA evaluation [14]. In support of this, using low-field extremity MRI, Savnik et al. [15] achieved a diagnostic accuracy for synovitis, bone edema, and bone erosion in RA comparable to that of high-field MRI.

Crues et al. [16] further reported that low-field dedicated-extremity MRI is more sensitive for detecting erosive changes in RA than radiography. In patients followed over 8 months, 30% demonstrated an increase in the size or number of erosions by MRI, while radiography revealed changes in only 0.8% of the patient cohort. Low-field dedicated-extremity MRI retains adequate imaging performance, but at a lower cost and with greater comfort and convenience for the patient. However, a limitation of low-field MRI is that the FOV is too small to enable an assessment of the hands and wrists in one examination. As wrist to PIP joints are usually affected in RA, examining the wrist to hand in one sequence is important for diagnosing and monitoring RA. Another disadvantage is that low-field MRI systems are not practical for small clinics to install because of their size and weight. To address these limitations and to render MRI more useful for RA diagnosis and treatment, we have developed a new low-field extremity MRI. This system has a large enough FOV to assess wrist to PIP joints in one examination, is lighter than its predecessor, and requires less total area to install.

The general adoption of MRI in general practice has also been hindered by a second problem. Many studies have used the RAMRIS OMERACT scoring method for MRI evaluation. However, this scoring method is too complex for use in daily medical examinations and treatments. We have used a new scoring system, cMRIS, for evaluating disease activity in RA patients treated with anti-TNF biologics. This method evaluates bone erosion, bone edema, and synovitis as well as RAMRIS. The RAMRIS scored bone erosion on a scale of 0–10 by its volume, which may be inconvenient. In addition, the RAMRIS method requires 2-D analysis. Therefore, we have improved this point and developed cMRIS. The cMRIS scores bone erosion on a scale of 0–3 by its volume, just as the method used for edema and synovitis. Considering the irreversibility of each finding, we decided that the coefficients for each finding should be 1.5 for bone erosion, 1.25 for bone edema, and 1 for synovitis. Based on the positive correlation that we obtained between ΔDAS28 and ΔcMRIS, we consider our scoring system to be useful in linking MRI image evaluation to clinical evaluation. However, a future large-scale study will be necessary to examine whether these coefficients are appropriate. Another problem is that synovitis cannot be evaluated precisely because we did not use gadolinium enhancement in our MRI system. As gadolinium enhancement requires intravenous injection and may induce severe side effects, such as nephrogenic systemic fibrosis, it cannot always be used in daily practice, especially in a small clinic. The problem of inaccuracy due to not using gadolinium can be

solved to some extent through the acquisition of experience. As the aim of our study was to establish the evaluation of RA disease activity by MRI in daily practice, we did not use gadolinium enhancement and instead developed an easier system to image and to facilitate the evaluations of these images.

In almost all patients, a positive correlation was observed between ΔDAS28 and ΔcMRIS. However, one patient in the IFX group showed a worsening of bone destruction when evaluated by cMRI even though the estimated DAS28–CRP indicated clinical remission. Prior to treatment, this patient had moderate disease activity (DAS28–CRP 4.1). She then responded well to the treatment and remained close to clinical remission during the study. The MRI scan showed a DAS28–CRP of 2.66 at the first imaging and 2.83 at the second imaging. However, both bone edema and erosion had worsened, as evidenced by the MRI scan. This patients provides good proof of how we can understand real disease activity using not only the DAS28 but also the cMRI in daily practice. In the future, rheumatologists should estimate real disease activity by MRI and other tools in addition to clinical activity as estimated by the DAS28.

Low-field extremity MRI has been reported to record a lower sensitivity than whole-body MRI in terms of bone edema assessment [17], and different sensitivities have been reported among different models [18]. We did not compare our cMRI image and the 1.5-T whole-body MRI image. However, work is now ongoing to develop an improved system, the 0.3-T MRI machine, called the compacTscan, which will enable a higher resolution and sensitivity imaging, and a more precise diagnosis of RA. To date, we have compared the 0.3-T cMRI image and the 1.5-T whole-body MRI image in three patients and obtained almost the same results (data not shown). The low-field extremity MRI is convenient for both patients and rheumatologists, and its use in daily practice could assist clinicians both in making an earlier diagnosis of RA and a more precise estimation of disease activity. The hope is that joint prognosis of RA patients will be improved using cMRI.

In conclusion, the results of our study have shown a positive correlation between ΔcMRIS and ΔDAS28, suggesting that cMRI and the cMRIS are useful for estimating total disease activity and joint damage in RA.

References

1. Cush JJ. Early rheumatoid arthritis—is there a window of opportunity? J Rheumatol Suppl. 2007;80:1–7.
2. Klarlund M, Ostergaard M, Jensen KE, Madsen JL, Skjødt H, Lorenzen I. Magnetic resonance imaging, radiography, and scintigraphy of the finger joints: one year follow up of patients with early arthritis The TIRA Group. Ann Rheum Dis. 2000;59:521–8.
3. McQueen FM, Stewart N, Crabbe J, Robinson E, Yeoman S, Tan PL, et al. Magnetic resonance imaging of the wrist in early rheumatoid arthritis reveals progression of erosions despite clinical improvement. Ann Rheum Dis. 1999;58:156–63.
4. Taylor PC. The value of sensitive imaging modalities in rheumatoid arthritis. Arthritis Res Ther. 2003;5:210–3.
5. Ostergaard M, Szkudlarek M. Imaging in rheumatoid arthritis—why MRI and ultrasonography can no longer be ignored. Scand J Rheumatol. 2003;32:63–73.
6. Haavardsholm EA, Bøyesen P, Østergaard M, Schildvold A, Kvien TK. Magnetic resonance imaging findings in 84 patients with early rheumatoid arthritis: bone marrow edema predicts erosive progression. Ann Rheum Dis. 2008;67:794–800.
7. Taouli B, Zaim S, Peterfy CG, Lynch JA, Stork A, Guermazi A, et al. Rheumatoid arthritis of the hand and wrist: comparison of three imaging techniques. AJR Am J Roentgenol 2004;182:937–43.
8. Savnik A, Malmskov H, Thomsen HS, Bretlau T, Graff LB, Nielsen H, et al. MRI of the arthritic small joints: comparison of extremity MRI (0.2 T) vs high-field MRI (1.5 T). Eur Radiol. 2001;11:1030–8.
9. Østergaard M, Peterfy C, Conaghan P, McQueen F, Bird P, Ejbjerg B, et al. OMERACT Rheumatoid Arthritis Magnetic Resonance Imaging Studies Core set of MRI acquisitions, joint pathology definitions, and the OMERACT RA-MRI scoring system. J Rheumatol. 2003;30:1385–6.
10. McQueen F, Lassere M, Edmonds J, Conaghan P, Peterfy C, Bird P, et al. OMERACT Rheumatoid Arthritis Magnetic Resonance Imaging Studies. Summary of OMERACT 6 MR Imaging Module. J Rheumatol. 2003;30:1387–92.
11. Klareskog L, van der Heijde D, Jager JP, Gough A, Kalden J, Malaise M, et al. Therapeutic effect of the combination of etanercept and methotrexate compared with each treatment alone in patients with rheumatoid arthritis: double-blinded randomized controlled trial. Lancet. 2004;363:675–81.
12. Brown AK, Quinn MA, Karim Z, Conaghan PG, Peterfy CG, Hensor E, et al. Presence of significant synovitis in rheumatoid arthritis patients with disease-modifying antirheumatic drug-induced clinical remission: evidence from an imaging study may explain structural progression. Arthritis Rheum. 2006;54:3761–73.
13. Martinez-Martinez MU, Cuevas-Orta E, Reyes-Vaca G, Baranda L, Gonzalez-Amaro R, Abud-Mendoza C. Magnetic resonance imaging in patients with rheumatoid arthritis with complete remission treated with disease-modifying antirheumatic drugs or anti-tumour necrosis factor alpha agents. Ann Rheum Dis. 2007;66:134–5.
14. Taouli B, Zaim S, Peterfy CG, Lynch JA, Stork A, Guermazi A, et al. Rheumatoid arthritis of the hand and wrist: comparison of three imaging techniques. AJR Am J Roentgenol.. 2004;182:937–43.
15. Savnik A, Malmskov H, Thomsen HS, Bretlau T, Graff LB, Nielsen H, et al. MRI of the arthritic small joints: comparison of extremity MRI (0.2 T) vs high-field MRI (1.5 T). Eur Radiol. 2001;11:1030–8.
16. Crues JV, Shellock FG, Dardashti S, James TW, Troum OM. Identification of wrist and metacarpophalangeal joint erosions using a portable magnetic resonance imaging system compared to conventional radiographs. J Rheumatol. 2004;31:676–85.
17. Bird P, Ejbjerg B, Lassere M, Østergaard M, McQueen F, Peterfy C, et al. A multireader reliability study comparing conventional high-field magnetic resonance imaging with extremity low-field MRI in rheumatoid arthritis. J Rheumatol. 2007;34:854–6.
18. Duer-Jensen A, Ejbjerg B, Albrecht-Beste E, Vestergaard A, Møller Døhn U, Lund Hetland M, et al. Does low-field dedicated extremity MRI (E-MRI) reliably detect RA bone erosions? A comparison of two different E-MRI units and conventional radiography with high resolution CT. Ann Rheum Dis. 2008. doi: 10.1136/ard.2008.093591.

Mod Rheumatol (2009) 19:366–371
DOI 10.1007/s10165-009-0174-0

ORIGINAL ARTICLE

Altered peptide ligands regulate type II collagen-induced arthritis in mice

Ei Wakamatsu · Isao Matsumoto · Yohei Yoshiga · Taichi Hayashi · Daisuke Goto · Satoshi Ito · Takayuki Sumida

Received: 4 March 2009 / Accepted: 2 April 2009 / Published online: 12 May 2009

Abstract We reported that peripheral blood mononuclear cells from HLA-DRB1*0101 Japanese patients with rheumatoid arthritis (RA) were highly reactive to 256–271 peptide of type II collagen (CII). Similar to RA, T cells reactive to CII (AA256–271) play a crucial role in the generation of arthritis in CII-induced arthritis mouse ($I\text{-}A^q$). In the present study, we regulated the CII reactivity of T cells from CIA mouse with $I\text{-}A^q$ by altered peptide ligand (APL). Eight different APLs were designed and screened for their antagonistic activity using CII reactive cytokine production assay. Four APLs of CII 256–271 exhibited antagonistic activity in CII-reactive T cells. Moreover, intraperitoneally injected APL-5 (G262A) significantly suppressed CII-induced arthritis in mice, whereas the other three APLs did not. Compared with the control, APL-5 suppressed interleukin (IL)-17 production by T cells from CII-induced arthritis mice. These results suggest that CII APL is a potentially suitable therapeutic strategy for the control of RA.

Keywords Altered peptide ligand · Antagonist · Type II collagen-induced arthritis · T cells

E. Wakamatsu is a research fellow of the Japan Society for the Promotion of Science.

E. Wakamatsu · I. Matsumoto · Y. Yoshiga · T. Hayashi · D. Goto · S. Ito · T. Sumida (✉)
Division of Clinical Immunology,
Doctoral Programs in Medical Sciences,
Major of Advanced Biomedical Applications,
Graduate School Comprehensive Human Science,
University of Tsukuba, 1-1-1 Tenodai,
Tsukuba, Ibaraki 305-8575, Japan
e-mail: tsumida@md.tsukuba.ac.jp

Introduction

Rheumatoid arthritis (RA) is an autoimmune disease characterized by persistent inflammatory synovitis leading to various degrees of cartilage destruction, bone erosion, and ultimately joint deformity and loss of joint function. Although the pathogenesis of RA is not clear, there is sufficient evidence to suggest the involvement of T cells in the inflammatory process, such as the infiltration of T cells, especially $CD4^+$ $CD45RO^+$ T cells, in joints of RA patients [1]. Furthermore, the susceptibility to RA is associated with HLA-DRB1 genes [2].

Type II collagen (CII), a molecule abundant in the articular cartilage, is considered one of the target autoantigens in RA. CII-reactive T cell clones have been established in vitro from synovial T cells of RA [3]. Sekine et al. [4] suggested that the expansion of oligoclonal T cells in RA joints is driven by stimulation of CII. Furthermore, the pathology in CII-induced arthritis (CIA) mice is similar to that in RA synovium. The susceptibility to CIA is determined by $I\text{-}A^q$, which is a major histocompatibility complex (MHC) class II molecule, and the immunodominant CII256–271 region of CII could be bound to $I\text{-}A^q$ molecules [5].

T cell activation depends on the ability of the T cell receptor (TCR) to recognize 8–20 amino acid peptides that are bound to MHC molecules. The process of recognition of peptides by TCR is flexible. If the amino acid residue of peptide ligands for TCR is substituted for a different amino acid and can still bind to the MHC molecules (altered peptide ligands, APLs), these APLs could regulate the activation of T cells. Several studies [6, 7] have shown that APL can potentially induce differential cytokine secretion, anergy, and antagonism of the response to wild-type antigens. Therefore, it is possible to use APL as a therapeutic

agent against T-cell-mediated diseases such as autoimmune diseases.

Our previous report [8] demonstrated that peripheral blood mononuclear cells from HLA-DRB1*0101 Japanese patients with RA were highly reactive to the 256–271 peptide of CII, and designed APLs suppressed T cell response to the immunodominant epitope (CII256–271) of CII. In the present study, we tried to regulate the CII-reactive T cells from CIA by eight different APLs to CII256–271. The results showed that four APLs could suppress the CII-reactive immune response in vitro and one APL exhibited an inhibitory effect on arthritis in vivo. These results suggest that the application of CII APL is a potentially suitable therapeutic strategy in the control of RA.

Materials and methods

Mice

DBA/1 J mice were purchased from The Charles River Laboratory (Yokohama, Japan). They were maintained in specific pathogen-free conditions in the laboratory animal resource center. All experiments were performed according to the *Guide for the Care and Use of Laboratory Animals* at Tsukuba University.

Induction of arthritis

Mice were immunized intradermally with 100 μg bovine type II collagen (CII: Collagen Research Center, Tokyo, Japan) in Complete Freund's adjuvant (CFA; Difco, Detroit, MI, USA). Each mouse received a booster dose on day 21 by intraperitoneal injection of 100 μg CII.

CII (256–271) peptide and altered peptide ligands

The peptide representing CII (AA256–271) and its altered peptide ligands (APL) containing specific amino acid substitutions were chemically synthesized by solid-phase procedure and purified by high-performance liquid chromatography (OPERON Biotechnologies, Tokyo).

Pre-pulse assay

Mice were immunized with 100 μg CII emulsified with CFA. Twelve days after immunization, the mice were anesthetized and the spleens removed. The spleen was treated with collagenase D (Roche, Mannheim, Germany), and $CD11c^+$ cells were isolated by CD11c microbeads (Miltenyi Biotec, Tokyo). The cells were pulsed with 50 μM CII256–271 peptides for 2 h. After washing, they were adjusted to 1×10^6 cells/ml and pulsed with 200 μM APLs for 12 h. On the other hand, $CD4^+$ cells were isolated using CD4 microbeads (Miltenyi Biotec) from splenocytes of mice immunized with CII. Then they were adjusted to 5×10^5 cells/ml and added to the plate where $CD11c^+$ cells were cultured for 12 h. The supernatants were collected 72 h later and interferon-γ (IFN-γ), IL-17, IL-2, IL-4, and IL-10 were measured by enzyme-linked immunosorbent assay (ELISA) (IL-17 and IL-2; BioLegend, San Diego, CA, IFN-γ, IL-4 and IL-10; eBioscience, San Diego, CA).

Treatment with APLs

Mice were treated with three injections each of 333 μg of APLs intraperitoneally (total 1 mg) on days 24, 26, and 28 after the first immunization with CII. The animals were observed at 3-day intervals and evaluated for the severity of arthritis by scoring each paw. The score ranged from 0 to 3 (0, no swelling or redness; 1, swelling or redness in one joint; 2, involvement of two or more joints; 3, severe arthritis of the entire paw and joints). The score of each animal was the sum of scores for all four paws.

Histopathology

The ankles were removed on day 60 after the first immunization with CII and fixed in 3% buffered formalin. The paws were decalcified in ethylenediaminetetraacetic acid (EDTA) in buffered formalin, embedded in paraffin, sectioned, and stained with hematoxylin and eosin.

Analysis of T cell response

Mice were treated with APLs by the above method. Their splenocytes were removed on day 35 after immunization, and $CD4^+$ cells and $CD11c^+$ cells were isolated by microbeads as described above. $CD4^+$ cells and $CD11c^+$ cells (5:1) were mixed and cultured with denatured CII (10 μg/ml), and supernatants were collected 24 h later. The amounts of IL-17 and IFN-γ were measured by ELISA.

Statistical analysis

The Mann–Whitney *U* test was used for statistical analysis. *P* values less than 0.05 denoted significant difference.

Results

Antagonistic activity of APLs in vitro

We designed eight different APLs as shown in Fig. 1a. We screened these APLs for their antagonistic activity

(A)

					P1	P2	P3	P4	P5	P6	P7	P8				
CII256-271	G	K	P	G	I	A	G	F	K	G	E	Q	G	P	K	G
APL-1	-	-	-	-	-	S	-	-	-	-	-	-	-	-	-	-
APL-2					-	D	-	-	-	-	-	-	-	-	-	-
APL-3	-	-	-	-	-	-	D	-	-	-	-	-	-	-	-	-
APL-4	-	-	-	-	-	-	K	-	-	-	-	-	-	-	-	-
APL-5	-	-	-	-	-	-	A	-	-	-	-	-	-	-	-	-
APL-6	-	-	-	-	-	-	-	-	A	-	-	-	-	-	-	-
APL-7	-	-	-	-	-	-	-	-	V	-	-	-	-	-	-	-
APL-8	-	-	-	-	-	-	-	-	M	-	-	-	-	-	-	-

(B)

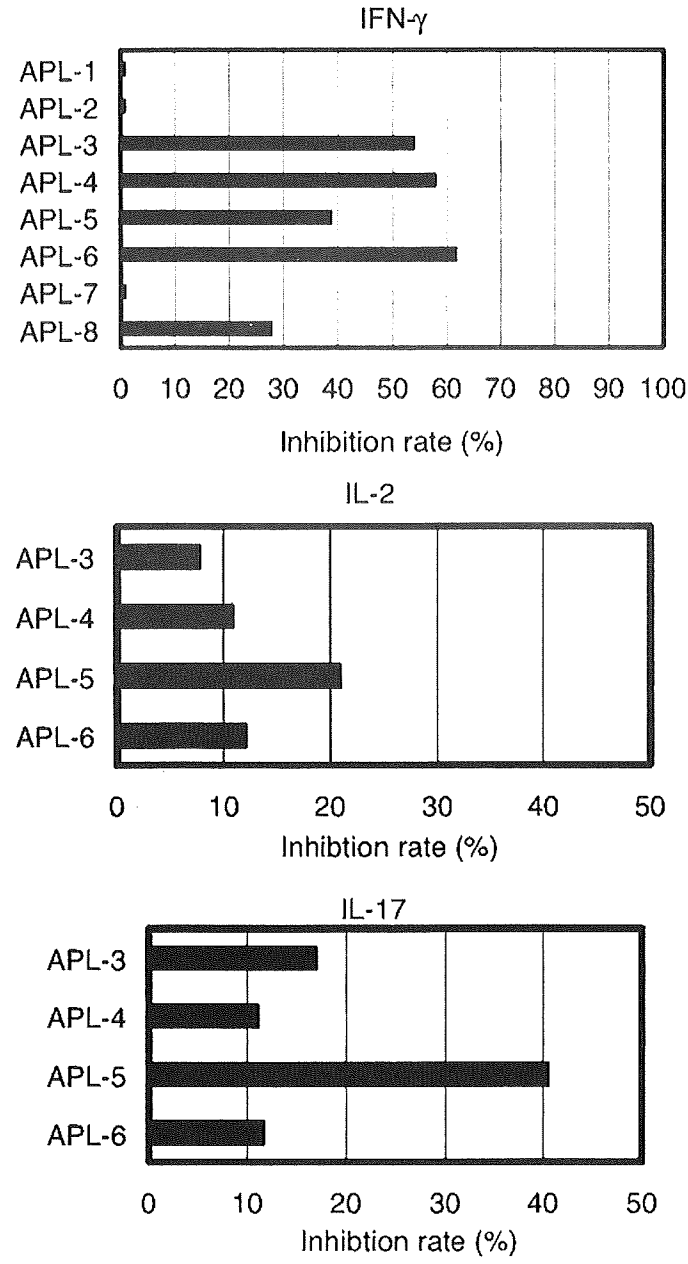

Fig. 1 Screening of APLs with antagonistic activity. **a** Altered peptide ligands were designed based on the I-A^q anchor motif. P1, P4, and P7 were predicted anchor position in CII256–271 peptide. **b** DBA/1 mice were immunized with CII. Antagonistic activity of APLs was investigated using CD4 T cells on day 12 after immunization by pre-pulse assay described in "Materials and Methods." Concentrations of IFN-γ, IL-2, and IL-17 were measured in the culture supernatants by ELISA. Inhibition rates of IFN-γ, IL-2 and IL-17 are expressed as percentage inhibition against the CII 256–271 peptide response. Data are representative of three similar experiments ($n = 3$)

using CII-reactive cytokine production assay. Four APLs (APL-3, -4, -5, and -6) suppressed (by more than 30–60%) production of CII256–271-reactive IFN-γ in vitro (Fig. 1b). We also investigated whether APL-3, -4, -5, and -6 suppressed the production of other cytokines. Similar to IFN-γ, the four APLs suppressed production of IL-2 and IL-17

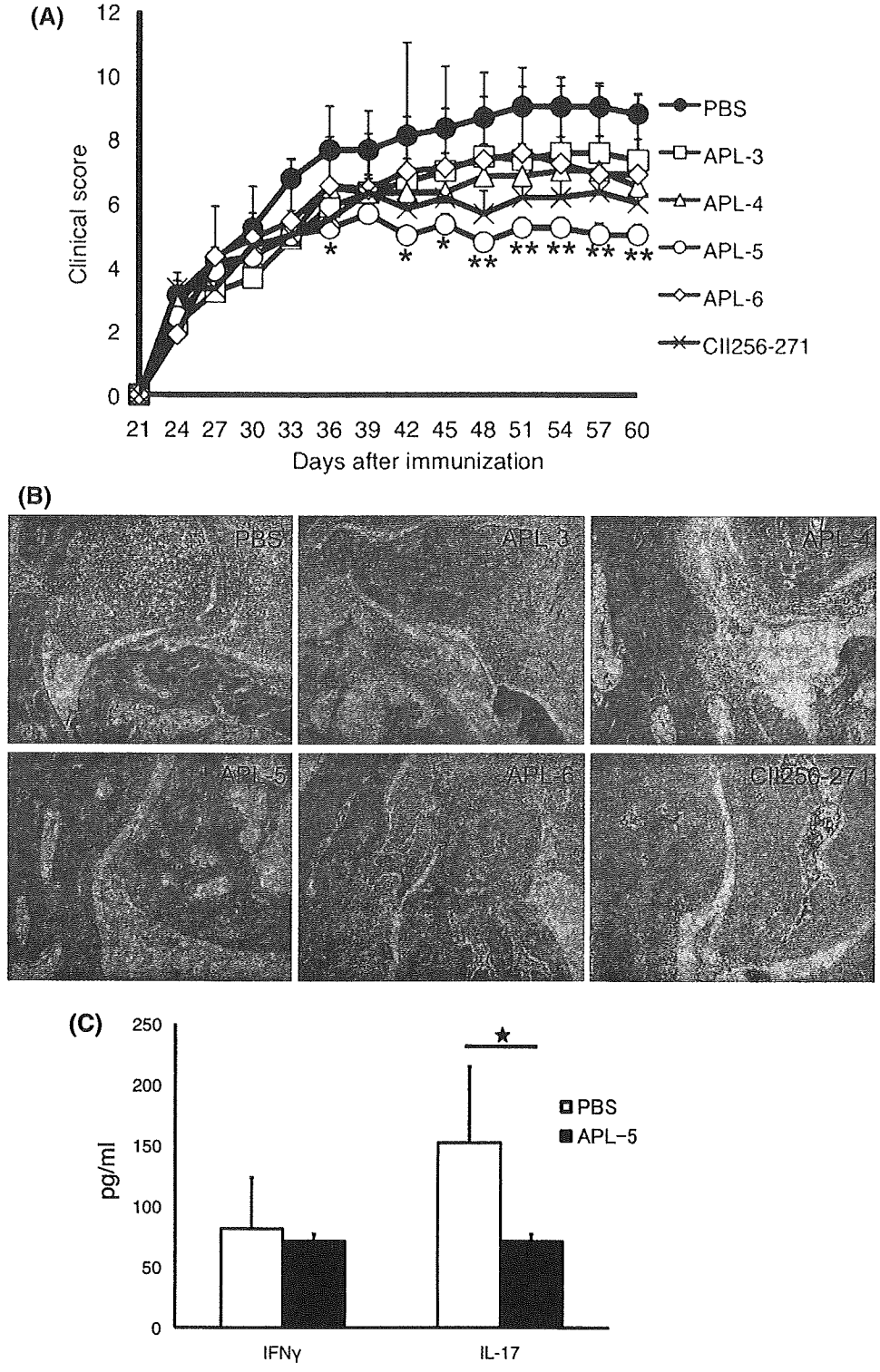

Fig. 2 Therapeutic effect of G262A in CIA. **a** DBA/1 mice were immunized and boosted with CII. Four APLs, CII256–271 peptide, and PBS were administered i.p. on days 24, 26, and 28 after immunization of CII (each $n = 9$), respectively. The clinical score of arthritis is expressed as mean ± standard error of the mean (SEM). $^{*}P < 0.01$, $^{**}P < 0.001$ versus PBS. **b** Each mouse was sacrificed on day 60 after immunization, and the ankles were examined by H&E staining. **c** On day 7 after the administration of APLs, $CD4^{+}$ T cells and dendritic cells were isolated from the spleen and co-cultured for 24 h. IFN-γ and IL-17 concentrations were measured by ELISA. T cell response of mice injected with PBS was assigned as 1. Data are mean ± standard deviation (SD) with triplicate culture. $^{*}P < 0.05$ versus PBS

(Fig. 1b). However, IL-4 and IL-10 were not detected in any samples (data not shown). Thus, we considered these four APLs as candidates for antagonistic APLs and used them in further experiments in vivo.

APL-5 results in significant suppression of arthritis

To investigate the therapeutic effects of the above four APLs on arthritis in vivo, we treated CII mice immunized

with APL intraperitoneally on day 24. CII256–271 peptide and phosphate-buffered saline (PBS) were injected as negative control. The results showed that APL-5 significantly suppressed the development of arthritis compared with the other three APLs ($P < 0.01$) and PBS ($P < 0.001$) (Fig. 2a). These mice were sacrificed on day 60 after immunization of CII, and histological examination was performed. As shown in Fig. 2b, APL-5 inhibited mononuclear cell infiltration compared with the other three APLs and PBS. These results indicate that CII-induced arthritis could be regulated by APL-5. T cell predominant epitope by itself (CII256–271) slightly decreased the severity of arthritis, suggesting activation-induced cell death by the excess dose of dominant epitope.

Effects of APLs on cytokine production

To examine whether APLs suppress CII-reactive T cells in vivo, we investigated the production of IFN-γ and IL-17 from CII-reactive T cells in APLs-treated mice. As shown in Fig. 2c, injection of APL-5 significantly suppressed IL-17 production, but not that of IFN-γ, by CII-reactive T cells ($P < 0.05$). The other APLs and CII256–271 peptides did not have any effects on the production of IFN-γ and IL-17 (data not shown).

Discussion

Several investigators [9–11] demonstrated the protective effects of APL using experimental autoimmune encephalomyelitis (EAE) and CIA. Co-immunization of mice bearing the H-2^u haplotype with an APL and an encephalogenic peptide prevented the development of EAE [9]. Furthermore, Myers et al. [10] showed that APL regulated the onset of CIA in H-2^q mice. Although their reports showed the protective activity of APL, the therapeutic effects of APLs have been hardly reported. Myers et al. [12] reported that administration of their APLs on day 28 after CII immunization decreased the incidence rate of arthritis though they did not show the score of arthritis of those mice. Zhao et al. [13] demonstrated that collagen-induced arthritis in rat was suppressed by oral administration of APLs after the onset of arthritis. These observations support the notion that their APLs might be a therapeutic strategy against arthritis. In the present study, administration of APL-5 after the onset of arthritis suppressed the development of CIA, indicating the therapeutic effect of APL on CIA. In contrast, Myers's study [12] administered APLs to CIA mice at the onset of arthritis. The experiments by Zhao et al. [13] were designed with oral administration and done using rat model. The most important message from this study is that APL-5 is common between CIA mice and patients with RA [8], indicating that clinical trial can be hoped for in the near future.

Several studies have examined the role of Th17 cells in CIA. Development of CIA was regulated in IL-17 knockout mice, suggesting that IL-17 plays a crucial role in arthritis [14]. Severe clinical and histologic CIA was induced in IFN-γ receptor knockout mice [15], whereas CIA was suppressed by the administration of anti-IFN-γ antibodies [16]. Therefore, the role of IFN-γ in the development of CIA is controversial. Our studies showed that APL-5 inhibited CII-reactive IL-17 production in vivo, suggesting the main contribution of IL-17 on the development of CIA.

Our experiments in vivo showed the possibility that each APL had different effect on T cell subset. APL-5 preferentially suppressed IL-17 but not IFN-γ; on the other hand, APL-6 suppressed IFN-γ but not IL-17. Although the precise mechanism is not clarified, these findings suggest that minor variations of the peptide may affect the peptide-binding affinity, or minor change of the physicochemical properties of amino acid residues may involve TCR binding activity.

In conclusion, the present study showed that administration of APL-5 suppressed the development of CIA in mice. CII APL is a potentially suitable therapeutic strategy for the control of RA.

Acknowledgment This work was supported in part by a Research Grant from the Ministry of Health, Labor, and Welfare, and the Research Grant from the Ministry of Education, Culture, Sports, Science, and Technology.

Conflict of interest statement All of the authors confirm that they have no conflicts of interest with regard to this work.

References

1. Struyk L, Hawes GE, Dolhain RJ, van Scherpenzeel A, Godthelp B, Breedveld FC, et al. Evidence for selective in vivo expansion of synovial tissue-infiltrating CD4+CD45RO+T lymphocyte on the basis of CDR3 diversity. Int Immunol. 1994;6:897–907.
2. Fugger L, Svejgaard A. Association of MHC and rheumatoid arthritis. HLA-DR4 and rheumatoid arthritis: studies in mice and human. Arthritis Res Ther. 2000;2:208–11.
3. Londei M, Savill CM, Verhoef A, Brennan F, Leech ZA, Duance V, et al. Persistence of collagen type II-specific T cell clones in the synovial membrane of a patient with rheumatoid arthritis. Proc Natl Acad Sci USA. 1989;86:636–40.
4. Saeki T, Kato T, Masuko-Hongo K, Nakamura H, Yoshino S, Nishioka K, et al. Type II collagen is a target antigen of clonally expanded T cells in the synovium of patients with rheumatoid arthritis. Ann Rheum Dis. 1999;58:446–50.
5. Luross JA, Williams NA. The genetic and immunopathological processes underlying collagen-induced arthritis. Immunology. 2001;103:407–16.
6. Magistris MTD, Alexander J, Coggeshall M, Altman A, Gaeta FC, Grey HM, et al. Antigen analog-major histocompatibility

complexes act as antagonists of the T cell receptor. Cell. 1992;68:625–34.
7. Pfeiffer C, Stein J, Aouthwood S, Ketelaar H, Sette A, Bottomly K. Altered peptide ligands can control CD4 T lymphocyte differentiation in vivo. J Exp Med. 1995;181:1569–74.
8. Ohnishi Y, Tsutsumi A, Matsumoto I, Goto D, Ito S, Kuwana M, et al. Altered peptide ligands control type II collagen-reactive T cells from rheumatoid arthritis patients. Mod Rheumatol. 2006;16:226–8.
9. Wraith DC, Smilek DE, Mitchell DJ, Steinman L, McDevitt HO. Antigen recognition in autoimmune encephalomyelitis and the potential for peptide-mediated immunotherapy. Cell. 1989;59:247–55.
10. Myers LK, Rosloniec EF, Seyer JM, Stuart JM, Kang AH. A synthetic peptide analogue of a determinant of type II collagen prevents the onset of collagen-induced arthritis. J Immunol. 1993;150:4652–8.
11. Miller SD, Turley DM, Podojil JR. Antigen-specific tolerance strategies for the prevention and treatment of autoimmune disease. Nat Rev Immunol. 2007;7:665–77.
12. Nakae S, Nambu A, Sudo K, Iwakura Y. Suppression of immune induction of collagen-induced arthritis in IL-17-deficient mice. J Immunol. 2003;171:6173–7.
13. Myers LK, Tang B, Rosloniec EF, Stuart JM, Chiang TM, Kang AH. Characterization of a peptide analogue of a determinant of type II collagen that suppress collagen-induced arthritis. J Immunol. 1998;161:3589–95.
14. Zhao J, Li R, He J, Shi J, Long L, Li Z. Mucosal administration of an altered CII263–272 peptide inhibits collagen-induced arthritis by suppression of Th1/Th17 cells and expansion of regulatory T cells. Rheumatol Int. 2008;29:9–16.
15. Vermeire K, Heremans H, Vandeputte M, Huang S, Billiau A, Matthys P. Accelerated collagen-induced arthritis in IFN-gamma receptor-deficient mice. J Immunol. 1997;158:5507–13.
16. Coppieters K, Van Beneden K, Jacques P, Dewint P, Vervloet A, Vander Cruyssen B, et al. A single early activation of invariant NK T cells confers long-term protection against collagen-induced arthritis in ligand-specific manner. J Immunol. 2007;179:2300–9.